

Nematic–isotropic transition in polydisperse systems of infinitely thin hard platelets

Martin A. Bates and Daan Frenkel

FOM Institute for Atomic and Molecular Physics, Kruislaan 407, 1098 SJ Amsterdam, The Netherlands

(Received 27 October 1998; accepted 16 December 1998)

We study the phase behavior of model colloidal systems composed of infinitely thin hard platelets, with polydispersity in the size of the particles. Semi-grand Gibbs ensemble simulations are used to study the coexisting nematic and isotropic phases for a range of systems with varying polydispersity. Particle size segregation is observed in the two coexisting phases, with the larger particles tending to be found in the nematic phase. This fractionation becomes more evident with increasing polydispersity. We examine the relationship between the size of a particle and its orientation in the nematic phase and find that the larger particles tend to be more orientationally ordered than the smaller ones. The coexistence densities determined from the simulations are compared to those obtained from recent experiments on colloidal platelets. © 1999 American Institute of Physics. [S0021-9606(99)51511-0]

I. INTRODUCTION

Dispersions of anisometric colloidal particles have long been known to exhibit an orientationally ordered nematic phase above a certain concentration and this phenomenon has now been observed for a wide variety of suspensions of rod shaped particles.¹ While numerous experimental, theoretical and simulation studies have been devoted to understanding the mesophase behavior of elongated colloidal particles,^{1–6} much less attention has been given to suspensions composed of disk shaped particles. However, computer simulations of infinitely thin platelets⁷ and other models of disks with finite thickness^{4,8} have shown that entropy driven transitions to liquid crystalline phases are possible for these systems. Onsager's theoretical approach of truncating the equation of state at the second virial coefficient has also been applied to disk models⁹ but, as pointed out by Onsager, while this approximation is valid for infinitely thin needles, it cannot be justified for infinitely thin disks.³ The reason that only a small number of studies of model colloidal platelets have been performed most probably stems from the fact that the observation of nematic phases in real colloidal systems of disk shaped particles is much rarer than for their rod counterparts. For example, the widely studied platelet systems composed of clay particles are typically found not to exhibit a nematic phase but rather a gel, although orientational order may exist at a local level in these systems.^{10,11} Nevertheless, the colloidal suspensions of sterically stabilized gibbsite platelets synthesized recently by van der Kooij and Lekkerkerker do appear to exhibit a nematic phase.¹² However, there is a large discrepancy between the coexistence densities determined in these experiments and those in computer simulations of apparently similar model systems.⁸

One feature common to many synthetic systems but often neglected in simulation studies is polydispersity in size and shape. All previous simulation studies of hard body disk models have been performed on systems of particles of equal diameter.^{4,7,8} Thus comparison of the transition densities de-

termined from these simulations and those in real colloidal suspensions may not be appropriate. Indeed, for rod shaped particles, size polydispersity has been shown to have a large effect on the coexistence densities and even on the stability of the various liquid crystalline phases.^{13–15} Therefore, to provide new simulation data for comparison with experimental systems and to gain a better understanding of the influence of size polydispersity in colloids, we report simulation results for polydisperse platelet systems.

II. THE MONODISPERSE LIMIT

The limiting case of zero polydispersity is clearly an important reference system for our model colloid; in this limit, we have a system of infinitely thin hard platelets of equal diameter. Such systems are found to exhibit a nematic and an isotropic phase with no other liquid crystalline phases, such as a columnar, observed.⁷ This is because the columnar phase is only expected when the volume fraction of the disk shaped particles becomes appreciable which, for the infinitely thin platelet model, cannot occur at finite densities since the volume fraction is zero. More recent simulations employing a scaling argument which increases the vanishingly small volume of a disk to a finite value, do indeed show that infinitely thin disks exhibit a columnar phase.¹⁶ However, here we shall consider the effect of polydispersity on the nematic and isotropic phases only and, in particular, how size polydispersity changes the location of the transition between these two phases.

Eppenga and Frenkel determined the equation of state for monodisperse platelet systems of various sizes ($N=25, 50, 100, 400, 800$) using Monte Carlo simulations.⁷ The nematic–isotropic (NI) transition was found to be weakly first order and located at a density $\rho = N\sigma^3/V \approx 4$, where σ is the diameter of a disk (see Fig. 1). Neither an apparent jump in density nor any hysteresis in the equation of state was found and so the coexistence densities could not be determined using standard techniques.¹⁷ Thus a different route

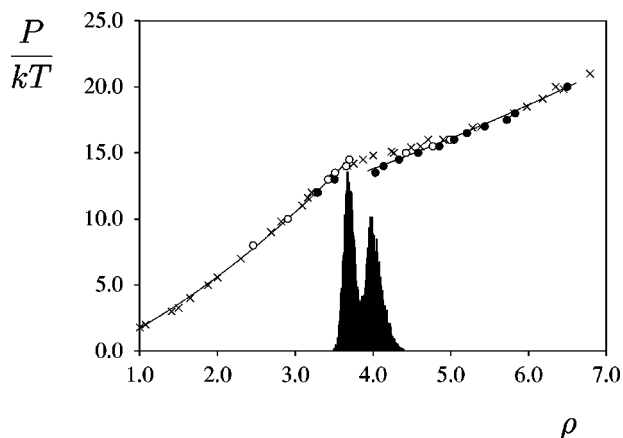


FIG. 1. Equation of state for monodisperse platelets determined from isobaric Monte Carlo simulations. Open circles: compression from isotropic phase, filled circles: expansion from nematic phase, crosses: data from Ref. 7. The histogram shows the probability $\text{Pr}(\rho)$ of observing a density $\rho = N\sigma^3/V$ in either phase in the Gibbs ensemble simulation.

was taken to locate the transition, by computing the chemical potential using Widom's insertion method¹⁸ at two different densities corresponding to the nematic and isotropic phases and then integrating the equation of state to determine the coexistence pressure; full details are given in the original article.⁷ This approach led to coexistence densities of $\rho_I = 4.04$ and $\rho_N = 4.12$. However, this method implicitly requires data of high accuracy for the equation of state because any small errors in its determination will affect the integration used to calculate the transition pressure and, therefore, the final values obtained for the coexistence densities. Since the monodisperse limit is an important reference point for the polydisperse model, we have performed new Monte Carlo simulations to locate the NI transition densities. Thus we have both recomputed the equation of state for a system of 1000 particles and simulated directly the two coexisting phases using a Gibbs ensemble simulation of 1600 particles.

The equation of state determined from isobaric Monte Carlo simulations is shown in Fig. 1, along with the results from the earlier study of infinitely thin platelets.⁷ Our results for the equation of state away from the transitional region are in good agreement with those determined previously. However, our results indicate clearly that the transition between the nematic and isotropic phases is first order and that the density jump at the transition is slightly larger than that determined previously. In comparison, the equation of state determined by Eppenga and Frenkel⁷ appears somewhat continuous in the transitional region. We note that very long runs of up to 500 000 cycles are necessary to obtain accurate statistics close to the transition because of slow fluctuations of the nematic order parameter and density. Presumably, such fluctuations in the density for smaller systems lead to the smoothing of the equation of state in the vicinity of the transition. The density jump and hysteresis in the equation of state is suggestive of a first order phase transition but, to obtain accurate values for the coexistence densities, a free energy calculation or thermodynamic integration is necessary.¹⁷ We attempted calculations to determine the Helmholtz free energy difference between an isotropic phase

at $\rho = 3.5$ and a nematic phase at $\rho = 4.5$ by applying a perturbation to the system so as to suppress the first order transition; this value was then used to calculate the Gibbs free energy difference between the two unperturbed phases as a function of pressure by integration of the equation of state.¹⁷ However, these calculations led to an unreasonable coexistence pressure, and therefore unreasonable coexistence densities, outside the observed hysteresis loop. Presumably, this method fails because of reasonably large fluctuations, leading to poor statistics, for the nematic order parameter as the transition is crossed by increasing the strength of the perturbation.

As an alternative method to determine the coexistence densities, we have performed a Gibbs ensemble simulation in which the two coexisting phases are studied simultaneously in separate boxes.¹⁹ Since the transition between the two phases is weak, the boxes change "identity" during the simulation. This means that a box which contains the isotropic (or nematic) phase at the start of the simulation may later be found to contain the nematic (or isotropic). To locate the transition, we therefore construct a histogram $\text{Pr}(\rho)$ of the probability to observe a density ρ in either phase.²⁰ This probability histogram is superimposed on the equation of state in Fig. 1. Even though the boxes switch identity during the simulation, the maxima in the probability histogram are still well defined and from these we determine the coexistence densities to be $\rho_I = 3.68 \pm 0.02$ and $\rho_N = 3.98 \pm 0.05$. We observe that the coexistence densities determined in this way are found to be within the hysteresis region of the equation of state obtained from the isobaric simulations.

III. THE POLYDISPERSE SYSTEMS

A. Simulation methodology

To study the properties of two phases of a pure substance at equilibrium, we must ensure that the temperature, pressure and chemical potential are equal in each phase; this can be achieved, for example, by using a Gibbs ensemble simulation.¹⁹ For a mixture of two or more components, the chemical potential of each component must be equal in each phase at equilibrium. This appears to rule out the possibility of studying phase equilibria in polydisperse systems characterized by a continuous distribution, such as particle size, since we must ensure chemical potential equality for an infinite number of species.²¹ The semi-grand canonical ensemble was introduced to overcome the difficulty of simulating polydisperse systems by imposing a chemical potential or activity distribution.²¹ By imposing the activity distribution, knowing the chemical potential of one species implies that the chemical potentials of all the species are known. Thus this ensemble differs from the canonical ensemble in that the identities of the particles are allowed to change during the simulation, subject to the imposed activity distribution. This method has been further extended to constant pressure and Gibbs ensemble variants.²² The constant volume and constant pressure variants have been employed successfully to study, for example, the influence of polydispersity on the freezing of hard spheres²³ and on the phase behavior of infinitely long rods at high density.¹⁵ The semi-grand Gibbs

ensemble, which we use to study the NI transition in our model colloidal system, is the choice method for directly simulating phase equilibria in polydisperse systems, since it allows us to perform a single simulation in which we can ensure equality of the temperature, pressure and chemical potentials of all species in both phases. We do note, however, that for this method to be efficient, the densities of the two coexisting phases must be low enough such that an adequate number of particle insertions can be accepted (as for any Gibbs ensemble simulation), in order to ensure the equality of chemical potentials in the two phases. The semi-grand Gibbs methodology is discussed in detail by Kofke and Glandt and we follow their scheme for generating and accepting trial moves.²²

Following other simulations using the semi-grand canonical ensemble or its variants,^{15,21–23} we choose the imposed chemical potential function for the disks to be

$$[\mu(\sigma) - \mu(\sigma_0)]/k_B T = -(\sigma - \sigma_0)^2/2\nu, \quad (1)$$

where $\mu(\sigma)$ is the chemical potential of a disk with diameter σ . We performed a series of simulations in which the width of the activity distribution $\nu^* = \nu/\sigma_0^2$ was fixed at different values. This leads to different composition distributions and thus allows us to determine the effect of varying the polydispersity in platelet systems.

Before discussing the results, we should briefly mention a few computational aspects of these simulations. Since it is the chemical potential function which is imposed and not the size distribution, we do not know the average size until after the simulation has finished.²¹ This means that it is not straightforward to choose a total volume for the two simulation boxes which corresponds to a point located in the two phase region, especially since the NI transition is typically weak in comparison to, for example, a gas–liquid transition. Thus a certain amount of trial and error was necessary to find a total volume for which the nematic and isotropic phases coexist. Moreover, while the particle exchange moves were found to be efficient (typically only 5000–10 000 trials were necessary to swap 5% of the particles), the volume exchange moves were slow and so density and nematic order parameter fluctuations were found to be sluggish. We note that volume moves are inefficient for hard body models, even at reasonably low densities, since there is high probability that any two particles are at or near contact and this significantly limits the size of the volume exchange trials. This means that rather long runs (often 250 000 cycles or more) were necessary to ensure equality of the pressure in the two simulation boxes. To monitor this during the simulation, we followed the graphical method described by Frenkel and Smit, in which the fraction of particles in box i ($x_i = N_i/N$) is plotted against the fraction of the total volume contained in box i ($y_i = V_i/V$) ($i = 1, 2$).²⁰ At coexistence, the simulation results should cluster around two points in the xy plane and so this method allows us to follow the equilibration of the system and determine when the pressure is equilibrated properly. We note that, as for the monodisperse case, the box identities were occasionally found to change and so the probability histogram $\text{Pr}(\rho)$ was used to determine the coexistence densities, although such changes were less frequently observed

in the polydisperse systems. In some cases, we found that the system would tend toward, for example, two (equivalent) isotropic phases; this, of course, implies that the total volume was too high to observe coexisting nematic and isotropic phases and so the total volume was decreased and the simulation restarted. Similarly, if two (equivalent) nematic phases were found, the total volume was increased. All simulations were performed using 1600 particles in total, as for the monodisperse system. If either box fell below 500 particles, the simulation was restarted using a different total volume.

An alternative scheme to study the coexisting nematic and isotropic phases would be to use a pseudo-Gibbs ensemble in which volume exchanges are never attempted;²⁴ this method avoids both the problems of one box becoming too small and the slow equilibration of the box sizes. Simulations in this ensemble are performed as follows (see Ref. 24 for practical details). Two simulations at different chemical potentials μ_I and μ_N , corresponding to a known stable point within each phase, are performed to obtain accurate values of the density and pressure at the specified chemical potentials. Once these are known, an estimate for the equilibrium chemical potential μ_{eq} can be obtained, since we can calculate the slope of each branch of the equation of state, $d\mu/dP = 1/\rho$. Two new simulations are then performed at $\gamma\mu_I + (1 - \gamma)\mu_{\text{eq}}$ and $\gamma\mu_N + (1 - \gamma)\mu_{\text{eq}}$ with $0 < \gamma < 1$ to obtain a refined estimate for μ_{eq} and the method iterated until convergence of the chemical potential and pressure is obtained. This method, therefore, determines the equation of state in the $P - \mu$ plane, starting from two points either side of the transition and gradually converges (depending on the value of γ) toward the transition. Such simulations were attempted for a monodisperse system but were found not to be stable after two or three iterations. The reason for this failure is probably due to the fact that the gradients of the two branches of the equation of state in the vicinity are similar⁷ and any inaccuracy in the pressure calculation at an individual point will lead to the prediction for the equilibrium chemical potential to be outside the range known to contain the transition. In addition, since the equation of state for infinitely thin disks in the $P - \mu$ plane does not show a large discontinuity in slope at the transition,⁷ many iterations would be necessary to obtain the coexistence densities with the same accuracy as those obtained by the isobaric simulations or the standard Gibbs ensemble technique. Thus pseudo-Gibbs ensemble simulations were not attempted for the polydisperse systems.

B. Composition distributions at coexistence

The composition distributions $f(\sigma)$ for the coexisting isotropic and nematic phases are shown for three simulations ($\nu^* = 0.01, 0.02, 0.03$) in Fig. 2, calculated from semi-grand Gibbs ensemble runs of 50 000 cycles during which time the box identities did not change. As in other semi-grand simulations of hard particles,^{15,23} the composition distributions are found to be shifted toward lower values of σ with respect to the center of the activity distribution at σ_0 . This occurs since large particles are entropically less favorable than smaller ones, especially at high number densities.²³ To ease the comparison of the composition distributions found for

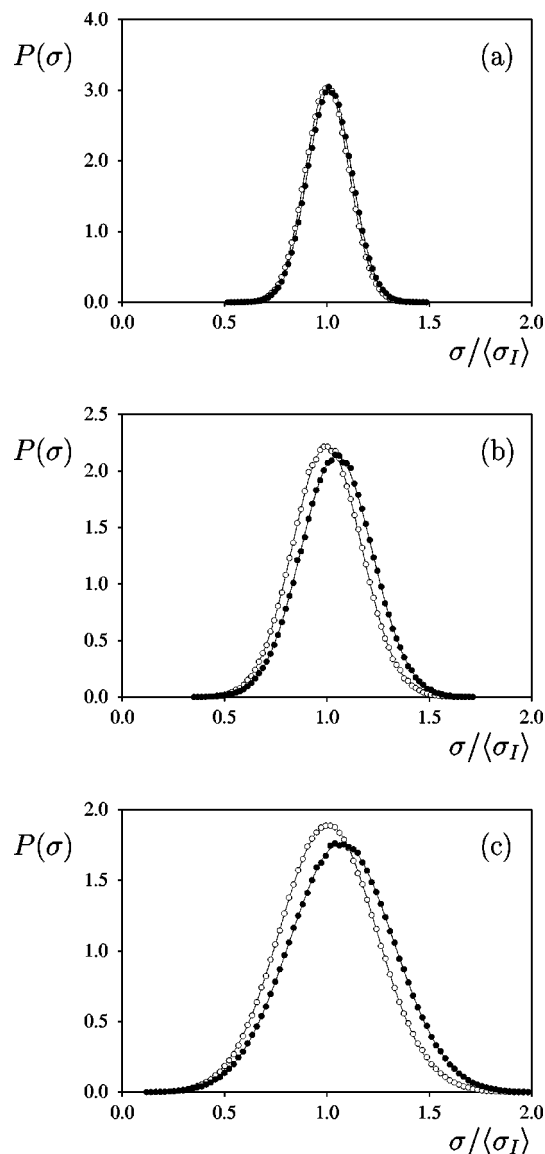


FIG. 2. Composition (size) distributions $f(\sigma)$ of the coexisting nematic and isotropic phases in the semi-grand Gibbs ensemble simulations with activity distribution widths $\nu^* = \nu/\sigma_0^2$ of (a) 0.01, (b) 0.02, and (c) 0.03. Open circles: isotropic, filled circles: nematic. The solid lines indicate the best fit Gaussian distribution to the simulation data. $\langle\sigma_I\rangle$ is the average diameter in the isotropic phase.

the different systems, we scale the particle sizes such that the average diameter in the isotropic phase is unity. Comparing the two composition distributions for each simulation, we find that the widths are essentially equal in the nematic and isotropic phases; for example, for the activity distribution of width $\nu^* = 0.03$, the standard deviation of the composition distribution in the nematic phase is 0.5% larger than that measured in the isotropic phase and so the difference in polydispersity in the two phases is negligible. However, the distribution in the nematic phase tends to be centered around a higher value than in the isotropic phase, indicating that, at coexistence, the average size of the particles is larger in the nematic phase, although not much so; for all polydispersities studied, there is a large overlap between the size distributions. We also observe that the size segregation becomes more apparent for the wider distributions, that is, for the

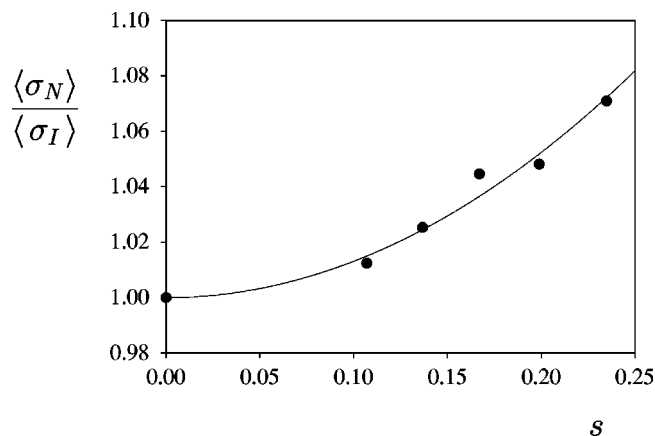


FIG. 3. Ratio of the average diameter in the nematic and isotropic phases as a function of polydispersity. The solid line is the best fit of a quadratic ($\langle\sigma_N\rangle/\langle\sigma_I\rangle = 1.0 + 1.3s^2$) to the simulation data (see text).

systems with higher polydispersity. This is highlighted in Fig. 3, where we plot the ratio of the average particle diameters in the nematic and isotropic phases as a function of polydispersity. For infinitely thin rods, this ratio is predicted to increase with the square of polydispersity;²⁵ this result also appears to hold for the data obtained from the simulations, albeit with a different prefactor (see Fig. 3). We note that the composition distributions are found to be essentially Gaussian and so we use their normalized standard deviation s as our measure of polydispersity.

C. Coexistence densities

We now turn to the coexistence densities of the two phases in the polydisperse systems. As we noted earlier, in the semi-grand simulations the particle sizes (diameters) are shifted to lower values compared to the imposed chemical potential distribution. As the particle sizes differ from one simulation to another of different polydispersity, for comparative purposes the number density $\rho = N/V$ is not so useful. Additionally, quantities such as volume fraction or packing fraction have no meaning for the model system, as the disks are infinitely thin. Thus, to compare the densities of the different systems, we use the dimensionless density defined by $\rho^* = \rho\langle\sigma^3\rangle$. This measure of the density is also available experimentally.¹² The coexistence densities $\rho_I^* = \rho_I\langle\sigma_I^3\rangle$ and $\rho_N^* = \rho_N\langle\sigma_N^3\rangle$ are shown as a function of polydispersity in Fig. 4. We note that in this plot, the differences in polydispersity in the two coexisting phases for each simulation are seen to be negligible, as stated earlier. We observe that polydispersity has a large influence on the location of the NI transition for the colloidal platelets. The major influence appears to be the widening of the coexistence region with increasing polydispersity. This feature is also predicted for bidisperse and polydisperse systems composed of rod shaped particles;^{1,13,25,26} the width of the coexistence region for rods is predicted to widen with the polydispersity squared.²⁵ Figure 4 indicates that a similar quadratic scaling gives a reasonable fit to the simulation data for disks. We also observe that, to a first approximation, the density ρ_I^* of the isotropic phase at the NI transition is essentially unchanged with in-

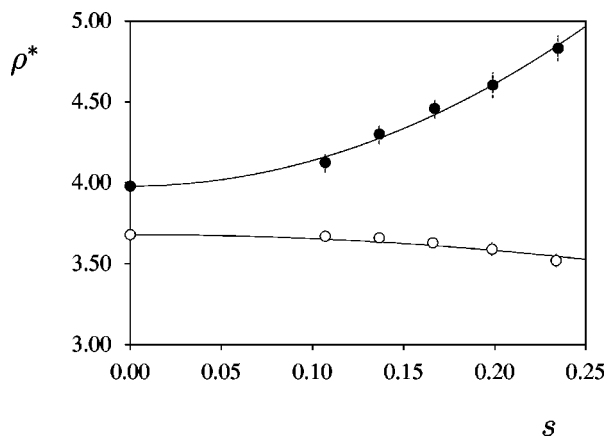


FIG. 4. Coexistence densities of the nematic and isotropic phases obtained from the semi-grand Gibbs ensemble simulations as a function of polydispersity s . The dimensionless densities are defined as $\rho_I^* = \rho_I \langle \sigma_I^3 \rangle$ and $\rho_N^* = \rho_N \langle \sigma_N^3 \rangle$. Open circles: isotropic, filled circles: nematic. The solid lines indicate the best fit of a quadratic to the simulation data for each phase, $\rho_I^* = 3.68 - 2.43s^2$ and $\rho_N^* = 3.98 + 15.82s^2$ (see text).

creasing polydispersity while that of the nematic increases strongly. This observation is in opposition to that found for rods, where polydispersity is found to shift the coexistence region to lower density.^{1,13,26} However, this comparison is not strictly appropriate because of the different scaling for the densities.

We note that our scaling of the coexistence densities implies that the scaled pressure of each phase is not equal, since we scale the pressure in the isotropic phase by $\langle \sigma_I^3 \rangle$ and that in the nematic by $\langle \sigma_N^3 \rangle$. This is entirely reasonable and can be explained in the following way (see Ref. 25 for a comparable situation). For a given size distribution $f(\sigma)$, the isotropic phase is stable up to a pressure P_I , at which the nematic phase first appears. As the pressure is further increased, the two phases coexist and the composition distributions rearrange themselves in such a way that the total distribution is $f(\sigma)$, but the distributions in the isotropic and nematic phases are $f_I(\sigma)$ and $f_N(\sigma)$ as shown in Fig. 2. At a

higher pressure P_N the isotropic phase is no longer stable and the nematic has the distribution $f(\sigma)$. Thus the scaling implicitly requires that the size distribution in both phases outside the transitional region is equivalent, as would be the case in an experimental system, where the total composition does not change on crossing the transition, but the composition of each phase need not be the same. This argument is not valid in general but is appropriate for our model system since the polydispersity and, therefore, the width of the distribution is found not to change significantly at the transition.

D. Orientational order—size distributions

Computer simulation allows us to investigate properties of a system which cannot easily be observed in experiments. Thus, while the size distributions can be obtained by extracting material from each phase and observing these using transmission electron microscopy,¹² all information about the orientational order of the different size particles is lost. To investigate how the size of a particle affects its orientational order in the nematic phase, we have calculated the singlet orientational distribution function (SODF) $f_\sigma(\beta)$ as a function of particle size, where β is the angle between the symmetry axis of the particle and the director and the subscript σ indicates that this function is calculated for a particular diameter. This is shown in Fig. 5(a) for the simulation with activity distribution of width $\nu^* = 0.03$. We observe that for large particles, the SODF is narrow and strongly peaked at $\cos \beta = 1.0$, indicating that these particles are essentially aligned along the director. For smaller particles, the distribution becomes wider although it remains peaked at $\cos \beta = 1.0$. This implies that the orientational order decreases with decreasing diameter. For the smallest particles, the SODF is almost flat, indicating that there is essentially no preferential alignment of very small particles. An alternative distribution which contains complementary information is the size distribution $f_\beta(\sigma)$, where the subscript β indicates that the distribution is calculated for a particular angle with respect to the nematic director; this is shown in Fig. 5(b). We

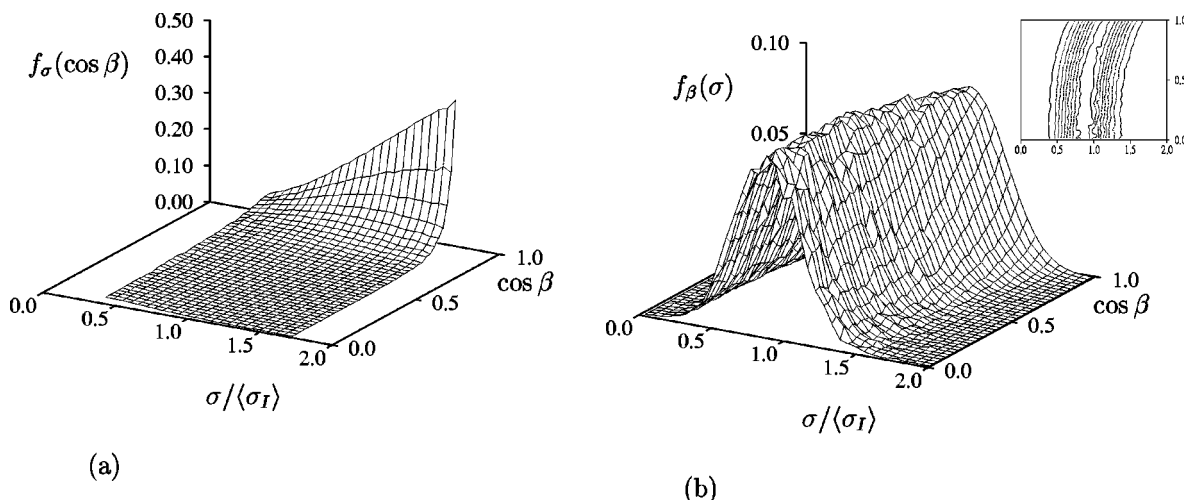


FIG. 5. (a) The singlet orientational distribution function $f_\sigma(\cos \beta)$ as a function of the particle diameter and (b) the size distribution $f_\beta(\sigma)$ as a function of angle for the nematic phase with an activity distribution width $\nu^* = \nu/\sigma_0^2$ of 0.03 (see text for definitions). $\langle \sigma_I \rangle$ is the average diameter in the isotropic phase. The inset in (b) shows the contour plot of $f_\beta(\sigma)$.

observe that, while the width of the distribution is not dependent on the angle made with the director, the average size of a particle is larger for smaller angles. This feature is highlighted in the contour plot in Fig. 5(b).

E. Comparison with experiment

Having determined the phase behavior of the model polydisperse disks, we can make an appropriate comparison with the experimental results obtained for gibbsite particles by van der Kooij and Lekkerkerker.¹² The aspect ratio of the gibbsite particles, including the grafted polymer chains which give the particles their steeply repulsive interactions, was determined to be 11:1, while the normalized standard deviation in diameter was calculated to be 0.25.¹² The volume fractions of the coexisting nematic and isotropic phases, converted to dimensionless densities, turn out to be $\rho_I^* = 2.5$ and $\rho_N^* = 2.7$. In comparison, for the model system at $s = 0.25$, we would expect the coexistence densities to be $\rho_I^* \approx 3.5$ and $\rho_N^* \approx 5.0$ (see Fig. 4). We observe a large discrepancy between the simulation and experimental data; thus the density at which the transition occurs in the experimental system is approximately half that in the simulation and the density jump at the transition is much smaller in the real system than in the model system, these values being 8% and 35%, respectively.

Clearly there are a number of features of the experimental system which are missing in the model and we may wonder which of these are dominant and lead to the large shift of the coexistence densities. The gibbsite particles are not circular but hexagonal and slightly irregular in shape. However, their deviation from the ideal shape appears minor and we would expect this not to have a large influence on the NI transition, but only on the structure of highly ordered phases at high densities when packing effects become important. While we cannot speculate quantitatively how the behavior of hexagons would differ from that of circular disks, if the effective average diameter is larger for hexagons than for the equivalent disks, then this will lead to a shift to lower values for the coexistence densities; the influence of particle shape will be addressed in a forthcoming paper.²⁷ However, even if this is so, it cannot explain the narrowing of the biphasic region. The gibbsite particles also have finite thickness (11:1 aspect ratio), whereas infinitely thin disks are considered in the model system. We again do not expect this to be a dominant factor, since the current and previous computer simulations indicate that the location of the NI transition is essentially equivalent for monodisperse disk systems of both finite and infinite aspect ratios; for cut spheres⁸ of aspect ratio 10:1, the NI transition is estimated to take place at $\rho_I^* = 3.81$ and $\rho_N^* = 3.87$ although, as in this work, the density gap may be found to differ slightly if a larger system is used to calculate the equation of state. Thus it appears that it is the face (possibly including the shape of the face²⁷) and not the thickness of the disk which is important in determining the low density phase behavior in the region of the NI transition. This is understandable when we consider that the nematic order parameter at the NI transition is typically only 0.45–0.55, indicating that the disks are far from perfectly aligned;

we expect the thickness to play a crucial role only for higher densities when the disks are almost parallel to each other and at close contact, such as at the transition to a columnar. The composition distributions in the experimental system are not Gaussian yet they are unimodal and not highly skewed.²⁸ Although these distributions are not equivalent in shape in the model and experimental system, it does not seem likely that small changes in the form of the distribution will lead to such large errors in the coexistence densities. A further feature which differentiates the model and experimental system is that the disks in the model are truly hard body, while there may be longer range attractions or repulsions present between the particles in the experimental system. The influence of such interactions is not clear and so we cannot speculate how these would change the phase behavior.

As a final important point, we note that no size segregation was observed in the coexisting phases in the experiments using gibbsite particles.¹² However, Fig. 2 clearly indicates that segregation is observed in the simulations, although the composition distributions of the coexisting phases do significantly overlap, even in the most polydisperse system. Since only 100 gibbsite particles are typically analyzed to determine the diameter distribution for each phase,²⁸ it is not possible to statistically distinguish the two distributions. Indeed, this is found to be the case if just 100 particles are picked at random from the coexisting phases in the simulations. This also means that it is not possible to accurately calculate the mean diameter or the higher moments of the distribution, which are crucial for the comparison of the experimental and simulation data, since we need to compare the dimensionless densities defined by $\rho^* = \rho \langle \sigma^3 \rangle$; in addition, $\langle \sigma^2 \rangle$ enters the expression to calculate the experimental number density from the volume fraction.¹² The use of the same values for the moments of the size distribution in each phase could account for the narrowing of the biphasic region for the gibbsite system. In addition, it is clear that any inaccuracy in the calculation of $\langle \sigma \rangle$ for each phase (and hence in $\langle \sigma^2 \rangle$ and $\langle \sigma^3 \rangle$) could lead to a shift in the coexistence densities ρ_I^* and ρ_N^* . We conclude that it is necessary to make an accurate determination of the size distribution of the gibbsite platelets to make a true comparison with the simulation results.

IV. CONCLUSIONS

We have performed semi-grand Gibbs ensemble simulations to investigate the influence of polydispersity on the NI transition in colloidal platelet systems. We find that the average diameter of particles in the nematic phase is slightly larger than that in the coexisting isotropic phase and that this size segregation increases with increasing polydispersity. In the nematic phase, the larger particles are found to have higher orientational order than smaller ones. The coexistence densities have been determined as a function of polydispersity and compared to those obtained from experimental observations of apparently similar platelets. Predictions from the simulation do not agree with the experimental coexistence densities. The differences between the systems are discussed; a possible explanation is that the platelets in the ex-

perimental system are not truly hard body particles but also interact through some longer range forces. However, the narrowing of the biphasic region in the experimental system could be due to the fact that size segregation was not observed and so the density scaling factor $\langle \sigma^3 \rangle$ was taken to be the same for each phase. The simulations reveal that size segregation does occur at the NI transition and, if this fractionation is taken into account for the experimental data, it leads to the widening of the coexistence region. This point can, of course, only be tested by a more accurate determination of the size distribution of the gibbsite particles. This would help us to decide whether or not longer range interactions are important in determining the phase behavior and so lead to a better understanding of the nature of the particles.

ACKNOWLEDGMENTS

The work of the FOM Institute is part of the research program of “Stichting Fundamenteel Onderzoek der Materie” (FOM) and is supported by the NWO (“Nederlandse Organisatie voor Wetenschappelijk Onderzoek”). M.A.B. acknowledges the financial support of the EU through the Marie Curie TMR Fellowship program. We are grateful to the authors of Ref. 12 for a preprint of their work and to I. Pagonabarraga and A. van Blaaderen for commenting on the manuscript.

¹P. A. Buining and H. N. W. Lekkerkerker, *J. Phys. Chem.* **97**, 11510 (1993) and references therein.

- ²S. Fraden, G. Maret, and D. L. D. Caspar, *Phys. Rev. E* **48**, 2816 (1993).
³L. Onsager, *Ann. (N.Y.) Acad. Sci.* **51**, 627 (1949).
⁴D. Frenkel and B. M. Mulder, *Mol. Phys.* **55**, 1171 (1985).
⁵D. Frenkel, H. N. W. Lekkerkerker, and A. Stroobants, *Nature (London)* **332**, 822 (1988).
⁶P. Bolhuis and D. Frenkel, *J. Chem. Phys.* **106**, 666 (1997).
⁷R. Eppenga and D. Frenkel, *Mol. Phys.* **52**, 1303 (1984).
⁸J. A. C. Veerman and D. Frenkel, *Phys. Rev. A* **45**, 5632 (1992).
⁹P. A. Forsyth, S. Marcelja, D. J. Mitchell, and B. W. Ninham, *J. Chem. Soc., Faraday Trans. 2* **73**, 84 (1977).
¹⁰A. Mourchid, A. Delville, J. Lambard, E. Lecolier, and P. Levitz, *Langmuir* **11**, 1942 (1995).
¹¹J.-C. P. Gabriel, C. Sanchez, and P. Davidson, *J. Phys. Chem.* **100**, 11139 (1996).
¹²F. M. van der Kooij and H. N. W. Lekkerkerker, *J. Phys. Chem.* **102**, 7829 (1998).
¹³H. N. W. Lekkerkerker, Ph. Coulon, R. van der Haegen, and R. Deblieck, *J. Chem. Phys.* **80**, 3427 (1984).
¹⁴A. M. Bohle, R. Holyst, and T. Vilgis, *Phys. Rev. Lett.* **76**, 1396 (1996).
¹⁵M. A. Bates and D. Frenkel, *J. Chem. Phys.* **109**, 6193 (1998).
¹⁶M. A. Bates and D. Frenkel, *Phys. Rev. E* **57**, 4824 (1998).
¹⁷D. Frenkel, in *Computer Simulation in Chemical Physics*, edited by M. P. Allen and D. J. Tildesley (Kluwer, Dordrecht, 1993).
¹⁸B. Widom, *J. Chem. Phys.* **39**, 2808 (1963).
¹⁹A. Z. Panagiotopoulos, *Mol. Phys.* **61**, 813 (1987).
²⁰D. Frenkel and B. Smit, *Understanding Molecular Simulation: From Algorithms to Applications* (Academic, San Diego, 1996).
²¹D. A. Kofke and E. D. Glandt, *J. Chem. Phys.* **87**, 4881 (1987).
²²D. A. Kofke and E. D. Glandt, *Mol. Phys.* **64**, 1105 (1988).
²³P. G. Bolhuis and D. A. Kofke, *Phys. Rev. E* **54**, 634 (1996).
²⁴F. A. Escobedo and J. J. de Pablo, *J. Chem. Phys.* **106**, 2911 (1997).
²⁵T. J. Sluckin, *Liq. Cryst.* **6**, 111 (1989).
²⁶G. J. Vroege and H. N. W. Lekkerkerker, *J. Phys. Chem.* **97**, 3601 (1993).
²⁷M. A. Bates, *J. Chem. Phys.* (submitted).
²⁸F. M. van der Kooij (private communication).